Asymmetric Miscibility in Random Copolymer/Homopolymer Blends: Monomeric Size and Polarity

Nicole N. Pellegrini

Department of Chemical Engineering, University of Pennsylvania, Philadelphia, Pennsylvania 19104

Karen I. Winey*

Department of Materials Science and Engineering, and Laboratory for Research in the Structure of Matter, University of Pennsylvania, Philadelphia, Pennsylvania 19104

Received July 15, 1999; Revised Manuscript Received October 29, 1999

ABSTRACT: A compositionally symmetric random copolymer of styrene and methyl methacrylate (S-*r*-MMA) was previously found to exhibit preferential miscibility with poly(methyl methacrylate) (PMMA) as compared with polystyrene (PS). This asymmetric miscibility of a random copolymer with its related homopolymers is not predicted by the Copolymer Effect theory, and its underlying causes are unclear in the absence of strong intermolecular interactions. In this paper, correlations were explored between asymmetric miscibility in random copolymer/homopolymer blends and the physical characteristics of the monomeric units. Four copolymer systems were studied, including S-*r*-MMA, which systematically varied the size and polarity of the monomeric units. A new technique, cross-sectional microscopy of thick bilayers, was developed to determine coexistence compositions in these blends based on linearized mass balances. In addition to S-*r*-MMA, a second compositionally symmetric random copolymer, poly(styrene-*ran*-ethyl methacrylate), was found to exhibit preferential miscibility with poly(ethyl methacrylate) over polystyrene. Two other copolymer systems, poly(styrene-*ran*-butyl methacrylate) and poly(styrene-*ran*-4 vinylpyridine), exhibit comparable miscibility with their related homopolymers. Comparing the monomer characteristics to both our miscibility and infrared spectroscopy results suggests that differences in the size and polarity of the monomeric units may induce asymmetric miscibility in random copolymers. Finally, deuteration within the S-*r*-MMA system was sufficient to eliminate the asymmetric miscibility behavior.

Introduction

The ability of random copolymers to promote mixing in otherwise immiscible polymer systems has led to widespread scientific and technological interest in these materials. One random copolymer that has been the subject of considerable investigation because of its unique miscibility behavior is poly(styrene-*ran*-methyl methacrylate) (S-*r*-MMA). DSC experiments first revealed that the compositionally symmetric $S_{0.48}$-*r*-MMA copolymer exhibited a wider range of miscibility with poly(methyl methacrylate) (PMMA) than with polystyrene (PS).[1] In a TEM ternary blend study, Winey and co-workers[2] observed that $S_{0.48}$-*r*-MMA is miscible with PMMA over a wider composition range than PS. Similarly, Kulasekere et al.[3] found asymmetric miscibility of S-*r*-MMA copolymer in binary blends with 85−99.5 wt % PS or PMMA, in that $S_{0.55}$-*r*-MMA was miscible with PMMA but completely immiscible with PS at these blend compositions. To date, S-*r*-MMA is the only copolymer that exhibits this asymmetric miscibility in the absence of specific interactions.

The preferential miscibility of a copolymer with one of its related homopolymers is of interest as current theoretical models of polymer miscibility do not predict this behavior. The Copolymer Effect (CE) theory,[4−6] an extension of the Flory−Huggins (FH) theory of polymer blends,[7] has generally succeeded in explaining the enhanced miscibility found in many systems containing random copolymers. According to this theory the χ interaction parameter for an A_xB_{1-x}/C_yD_{1-y} blend of copolymers can be determined from the weighted sum of its component monomer−monomer interaction parameters, χ_{ij}, as

$$\chi_{blend} = \sum_{i,j} C_{ij}\chi_{ij} \qquad (1)$$

The C_{ij} term is related to the number of contacts between monomers *i* and *j*, determined by the molar compositions of the blend components, and is positive for intermolecular interactions and negative for intramolecular interactions. A result of this theory is the prediction that a compositionally symmetric $A_{0.5}B$ copolymer should be equally miscible with its related A- and B-type homopolymers. Specifically, eq 1 yields χ_{blend} (or χ_{hc}) = $0.25\chi_{AB}$ for both the $A/A_{0.5}B$ and $B/A_{0.5}B$ homopolymer/copolymer blends. This conversely implies that if χ_{hc} is known for either A/A_fB or B/A_fB, χ_{AB} can be determined.

This relationship fails, however, for the $S_{0.48}$-*r*-MMA copolymer systems. The FH theory is used to determine homopolymer/copolymer interaction parameters for PS/$S_{0.48}$-*r*-MMA and PMMA/$S_{0.48}$-*r*-MMA from the coexistence compositions reported by Winey et al., yielding $\chi_{\text{PS}/\text{S}_{0.48}-r-\text{MMA}} = 0.0075$ and $\chi_{\text{PMMA}/\text{S}_{0.48}-r-\text{MMA}} = 0.0045$. Then applying CE theory to these values for χ_{hc} leads to $\chi_{\text{PS/PMMA}} = 0.028$ and $\chi_{\text{PS/PMMA}} = 0.020$. This significant disparity in $\chi_{\text{PS/PMMA}}$ indicates that interactions are present in the PS/PMMA/$S_{0.48}$-*r*-MMA system that are not being captured in the Copolymer Effect treatment.

In the absence of strong intermolecular interactions such as hydrogen bonding, the reasons for such deviation from predicted behavior are currently unclear. Theories and experiments have been proposed linking the magnitude of interaction parameters with various

---

* To whom correspondence should be addressed.

10.1021/ma991151t CCC: $19.00

monomeric physical attributes. Bates et al.[8] noted a correspondence between interaction strengths in polyolefin blends and the difference in statistical segment lengths of the component chains, Δl. This result was interpreted to mean that segmental mismatch decreases the entropy of mixing for a blend, causing a positive contribution to χ. Differences in the volume occupied by each monomer unit might also affect the packing of the polymer chains and hence miscibility in a similar fashion. Furthermore, solubility, related to the polarity of the molecules, could affect the miscibility of the copolymer with related homopolymers as the more polar monomeric units may favor interactions with similar polar units over nonpolar ones. The solubility parameters of two polymers have often been used to predict interaction parameters according to the equation

$$\chi = \frac{v}{RT}(\delta_A - \delta_B)^2 \tag{2}$$

where v is a reference volume and δ_A and δ_B are the solubility parameters of components A and B.[9] Graessley et al.[10] have investigated mixing behavior in blends of hydrocarbons and noted correlations between segment lengths and solubility parameters, but they also found inconsistencies between the interactions observed experimentally and those predicted by χ's estimated from solubility parameters.

In this paper, we investigate the miscibility behavior of several blends containing a homopolymer and a compositionally symmetric random copolymer. Our objective is to determine whether there is a correlation between the asymmetric miscibility behavior, as has been observed for the PS/PMMA/$S_{0.48}$-*r*-MMA system, and a mismatch in monomer size and/or polarity. The polymer systems chosen for this study have monomers that are structurally similar to styrene and methyl methacrylate, but vary in monomer size and polarity in a systematic fashion. We have developed a new technique which is a simplification of the TEM approach, cross-sectional microscopy of thick bilayers, to determine coexistence compositions in blends based on linearized mass balances. This technique is relatively simple, flexible, and inexpensive compared to other commonly employed experimental methods for studying miscibility in polymer systems. Furthermore, blend components do not need to be deuterated, as is required to achieve contrast for techniques such as forward recoil spectrometry (FRES) and small-angle neutron scattering (SANS). The Copolymer Effect theory is applied to the coexisting composition results of each system to determine whether and to what extent it displays asymmetric miscibility behavior, as indicated by $\chi_{AB}(A/AB) \neq \chi_{AB}(B/AB)$. Results suggest that both monomer packing and polarity effects may contribute to asymmetric miscibility in homopolymer/random copolymer blends. These experiments reveal a second homopolymer/random copolymer system that exhibits asymmetric miscibility similar to PS/PMMA/$S_{0.5}$-*r*-MMA. They also confirm the strong effect of deuteration on miscibility in the styrene/methyl methacrylate system reported separately.[11,12]

Experimental Section

Material. For this study, polymer systems were carefully selected so that the monomers are structurally similar to styrene and methyl methacrylate and allow us to investigate size and polarity effects in a systematic fashion. We also selected monomer pairs that exhibited copolymer sequencing statistics similar to styrene and methyl methacrylate, as differences in sequence distribution can strongly influence miscibility.[1,2,13,14] On the basis of these criteria, four systems were studied: (I) polystyrene/poly(methyl methacrylate)/poly(styrene$_{0.49}$-*ran*-methyl methacrylate), PS/PMMA/$S_{0.49}$-*r*-MMA; (II) polystyrene/poly(ethyl methacrylate)/poly(styrene$_{0.47}$-*ran*-ethyl methacrylate), PS/PEMA/$S_{0.47}$-*r*-EMA; (III) polystyrene/poly(butyl methacrylate)/poly(styrene$_{0.50}$-*ran*-butyl methacrylate), PS/PBMA/$S_{0.50}$-*r*-BMA; (IV) polystyrene/poly(4-vinylpyridine)/poly(styrene$_{0.50}$-*ran*-4 vinylpyridine), PS/P4VP/$S_{0.50}$-*r*-4VP.

Table 1. Materials Description

system		M_w	M_w/M_n	$r_1{}^{a-c}$	$r_2{}^{a-c}$	r_1r_2
I	PS-65	65 000	1.04	0.46	0.48	0.22
	PMMA	27 000	1.11			
	$S_{0.49}$−*r*−MMA	361 000	2.23			
II	PS-129	129 000	1.05	0.53	0.41	0.22
	PEMA	136 000	1.89			
	$S_{0.47}$−*r*−EMA	73 100	1.51			
III	PS-156	156 000	1.03	0.56	0.40	0.22
	PBMA	183 000	1.05			
	$S_{0.50}$−*r*−BMA	224 000	2.31			
IV	PS-8	8000	1.09	0.52	0.69	0.36
	P4VP	9800	1.11			
	$S_{0.50}$−*r*−4VP	127 000	2.79			
V	dPS	72 000	1.04	0.46	0.48	0.22
	dPMMA	33 900	1.11			
	$S_{0.49}$−*r*−MMA	361 000	2.23			

[a] *Copolymerization*; Hamm, G. E., Ed.; Interscience: New York, 1964. [b] Otsu, T.; Ito, T.; Imoto, M. *J. Polym. Sci., Part C* **1967**, *16*, 2121. [c] Tamikado, T. *J. Polym. Sci.* **1960**, *43*, 489.

We also studied the deuterated polystyrene (dPS)/deuterated poly(methyl methacrylate) (dPMMA)/$S_{0.49}$-*r*-MMA system in order to confirm our observations in separate FRES experiments that this deuterated system does not show the asymmetric miscibility that the hydrogenated polymer system does.[11]

The molecular weights and reactivity ratios for all five systems are listed in Table 1. The reactivity ratios, r_1 and r_2, are a measure of the sequencing statistics expected for a given monomer pair.[15] The fact that r_1 and r_2 are both <1 for all pairs indicates that each monomer radical reacts preferentially with the other. The product r_1r_2 describes the overall sequencing statistics of the chain. All systems have $r_1r_2 < 0.5$, which indicates that the random copolymers will be more alternating than statistically random in sequence.[16] Previous ^{13}C NMR characterization[1] on a compositionally symmetric S-*r*-MMA determined that only ~10% of triads in the copolymer occurred as homotriads, whereas a statistically random symmetric copolymer would have 25% of triads existing as homotriads. The $S_{0.49}$-*r*-MMA copolymer was synthesized via methods described previously[1] and is the same copolymer used in our FRES experiments on dPS/$S_{0.49}$-*r*-MMA and dPMMA/$S_{0.49}$-*r*-MMA miscibility.[11] $S_{0.47}$-*r*-EMA and PEMA were synthesized via similar free radical polymerizations. Copolymerizations were carried out to less than 5% conversions to avoid composition drift. The remaining homopolymers and copolymers were purchased from various commercial sources. The PS and PMMA used in system I were selected to match the molecular weights of the dPS and dPMMA used in system V to simplify direct comparison of the two systems. For systems II, III, and IV, homopolymer molecular weights for each system were matched closely to minimize molecular weight effects on miscibility. Using low molecular weights increases blend miscibility, but sample preparation becomes more difficult for most materials if the molecular weights are less than ~50 000.

Sample Preparation. Samples were prepared in a "partial overlap" geometry, as shown in Figure 1a, such that there are three distinct regions of each sample, from left to right: pure homopolymer, the homopolymer/copolymer bilayer, and pure copolymer. This geometry is used so that mass balance calculations can be performed based on thicknesses of the three

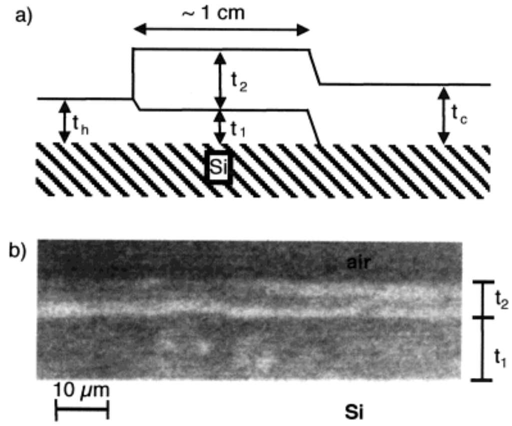

Figure 1. (a) Schematic cross-sectional view of a bilayer sample with partial overlap after annealing. Part a was drawn with an expanded vertical scale. (b) Image of a PMMA/$S_{0.49}$-*r*-MMA bilayer, after 15 days of annealing at 150 °C.

regions after annealing, t_h, t_1 and t_2, and t_c. For each homopolymer/copolymer pair, a minimum of three samples were prepared with varied overall homopolymer volume fraction by varying t_h and t_c (see eq 3). Films were doctorbladed from toluene, tetrahydrofuran, or methyl ethyl ketone solution onto either glass slides or silicon wafers. Only polymers of $M_w < 65\,000$ were doctorbladed directly onto silicon, as the dried films were too delicate to be scored and floated off glass. Dried individual films were 5−30 μm thick. The homopolymer was the first layer on the silicon wafer and the copolymer was the second layer, with the exception of the PBMA/$S_{0.50}$-*r*-BMA samples. Samples were annealed at 150 °C under vacuum, and cross-section fractures were taken for analysis after annealing periods of 7−53 days. Fractures were taken every ~7 days to determine when equilibrium conditions appeared to have been obtained.

Cross Sectional Microscopy and Analysis. Optical microscopy was employed for measuring cross-sectional layer thicknesses. These data were then converted into polymer coexistence compositions through mass balance relationships. Fracture surfaces were examined at 50 or 100× magnification. No staining or interfacial coating was necessary to differentiate between the polymer layers, as seen in the sample image of an annealed bilayer in Figure 1b. For each sample, four thicknesses were measured using a video monitor: the thicknesses of the pure homopolymer and copolymer layers, t_h and t_c, and the thicknesses in the annealed bilayer, t_1 and t_2. Generally 20−50 measurements were taken from each fracture surface, for each thickness, to obtain average values and to verify the consistency of the layer thicknesses. Data from samples where $t_h + t_c$ and $t_1 + t_2$ did not agree within 10% were discarded.

Analysis of the cross-sectional microscopy data begins with the conversion of measured layer thicknesses into polymer volume fractions. Similar to the TEM ternary blend study[2] of PS/PMMA/$S_{0.48}$-*r*-MMA discussed earlier, this is accomplished through application of stereology, which states that the volume fraction within a bulk sample is equal to the areal, line, or point fraction of a particular phase. Here we use line fractions based on the average layer thicknesses measured via optical microscopy, combined with mass balances, to extract the equilibrium phase compositions. The overall homopolymer volume fraction for each sample, ϕ_h, is obtained from the pure copolymer and homopolymer layer thicknesses as

$$\phi_h = \frac{t_h}{t_h + t_c} \tag{3}$$

Similarly, the volume fraction of the homopolymer-rich phase in the bilayer after annealing, Φ, is

$$\Phi = \frac{t_1}{t_1 + t_2} \tag{4}$$

A mass balance then relates ϕ_h and Φ to the equilibrium phase compositions, ϕ'_h and ϕ''_h:

$$\phi_h = \Phi\phi'_h + (1 - \Phi)\phi''_h \tag{5}$$

which is rearranged into a linear relationship between ϕ_h and Φ

$$\phi_h = (\phi'_h - \phi''_h)\Phi + \phi''_h \tag{6}$$

According to eq 6, plotting ϕ_h as a function of Φ for a given homopolymer/ copolymer system will yield ϕ'_h and ϕ''_h from the slope and intercept. The $\o_h$ vs Φ equilibrium data for all five systems are reported elsewhere.[17]

Infrared Spectroscopy. Reflective IR spectroscopy was performed on a Perkin-Elmer System 2000 infrared spectrometer, using powder samples of PMMA, $S_{0.49}$-*r*-MMA, $S_{0.47}$-*r*-EMA, and $S_{0.50}$-*r*-BMA. Our interest was in the carbonyl stretching region of the IR spectra for these materials, 1650−1800 cm^{-1}, to look for signs of polarity-driven molecular interactions.

Results

Coexistence compositions in the bilayer samples were observed to reach a steady value within 14−21 days of annealing. A sample ϕ_h vs Φ plot, for the PMMA/$S_{0.49}$-*r*-MMA system, is shown in Figure 2. The open circles represent data from the 7-day anneal, and filled circles, squares and triangles data from the 14-, 21-, and 32-day anneals. Multiple points at the same ϕ_{PMMA} represent data from the same staggered bilayer sample. Only results for anneals ≥14 days that agree within experimental error, were used in determining the mass balance line fit. Rather than compute diffusion times, we elected to experimentally determine appropriate anneal times in this fashion because we have not measured the diffusion coefficients for the four random copolymers used in this study. For the PMMA/$S_{0.49}$-*r*-MMA system shown in Figure 2, the equilibrium phase compositions were determined to be 11 and 93 vol % PMMA. The coexistence compositions determined for the other binary blends in systems I−IV are listed in Table 2.

To evaluate the accuracy of the cross-sectional microscopy technique, ϕ'_h and ϕ''_h determined for system V are listed in Table 3, along with the values determined for the same materials using FRES as reported elsewhere.[11] The determined equilibrium phase compositions agree within experimental error, although that error range is greater for the cross-sectional microscopy technique (0.6−0.15) than for FRES (0.003−0.05). The same trend is observed in the results obtained from both methods, in that $S_{0.49}$-*r*-MMA exhibits comparable miscibility with dPS and dPMMA, contrary to the asymmetric miscibility of this copolymer with PS and PMMA.

To compare the results for systems I−IV, interaction parameters are more useful than coexisting phase compositions, as ϕ'_h and ϕ''_h are molecular weight dependent and interaction parameters should not be. The Flory−Huggins theory was applied to calculate the homopolymer/copolymer interaction parameter, χ_{hc}, for each binary blend and then the Copolymer Effect theory was used to calculate the monomer/monomer interaction parameter, χ_{AB}, based on both the A/AB and B/AB blend results. The Flory−Huggins mean field, lattice-model theory of homopolymer blends describes the free energy

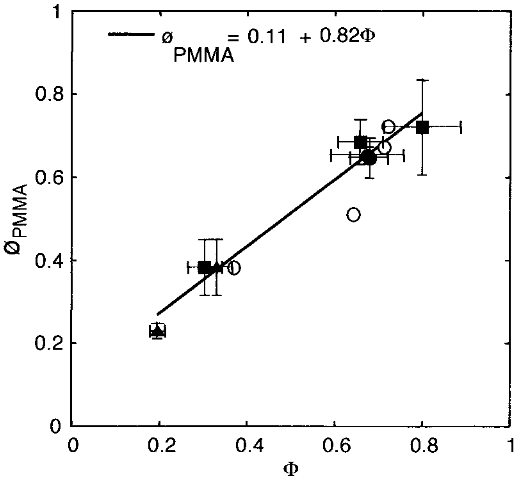

Figure 2. Microscopy results for PMMA/$S_{0.49}$-*r*-MMA samples. Open circles are data from 7-day anneals. Filled circles, squares, and triangles are data from 14-, 21- and 32-day anneals, respectively, which are used to determine the $ø_{PMMA}$ vs Φ line fit.

of mixing for a binary blend, in our case a homopolymer *h* and a copolymer *c*, as

$$\frac{\Delta G_m}{RT} = \frac{\phi_h}{N_h v_h}\ln\phi_h + \frac{\phi_c}{N_c v_c}\ln\phi_c + \frac{\chi_{hc}}{v}\phi_h\phi_c \qquad (7)$$

N_i is the number of monomers per chain of *i*, v_i is the volume per monomer of *i*, *v* is a reference volume (taken close to or equal to the smallest v_i) and χ_{hc} is the interaction parameter for the homopolymer/copolymer system. The equilibrium compositions ϕ_i' and ϕ_i'' correspond to the compositions where the chemical potential for the blend components, determined from the derivative of (7), is the same in both phases. Application of this equilibrium criteria yields

$$0 = \ln\left(\frac{\phi_h'}{\phi_h''}\right) + (\phi_h'' - \phi_h')\left(1 - \frac{N_h v_h}{N_c v_c}\right) + \frac{\chi_{hc}}{v}N_h v_h((1 - \phi_h')^2 - (1 - \phi_h'')^2) \qquad (8)$$

and

$$0 = \ln\left(\frac{1 - \phi_h'}{1 - \phi_h''}\right) + (\phi_h' - \phi_h'')\left(1 - \frac{N_c v_c}{N_h v_h}\right) + \frac{\chi_{hc}}{v}N_c v_c((\phi_h')^2 - (\phi_h'')^2) \qquad (9)$$

which can each be solved for χ_{hc} if ϕ_h' and ϕ_h'' are known. The values for χ_{hc} reported in Table 2 are the average of the two solutions to these equations. The difference between the experimentally measured coexistence compositions and those given by the best fit χ_{hc} averaged 3 vol %.[17]

Copolymer Effect theory was used to determine χ_{AB} from each χ_{hc}. Equation 1 is rearranged and solved for χ_{AB} as

$$\chi_{AB} = \chi_{hc}/(1 - f)^2 \qquad (10)$$

for the A/A_fB blends and

$$\chi_{AB} = \chi_{hc}/f^2 \qquad (11)$$

for the B/A_fB blends. The calculated χ_{AB}'s for systems I–IV are listed in Table 2. The $\chi_{PS/PMMA}$ values of 0.028 and 0.021, from the PS/$S_{0.49}$-*r*-MMA and PMMA/$S_{0.49}$-*r*-MMA blends respectively, are higher than the literature value of 0.018,[18] although the disagreement is smaller with the $\chi_{PS/PMMA}$ from the PMMA/$S_{0.49}$-*r*-MMA results. Interpretation of the PS/$S_{0.49}$-*r*-MMA results are complicated by the fact that the best fit χ_{hc} using eqs 8 and 9 for a blend changes rapidly as phase compositions approach 0 and 1. For example, using phase compositions of 0.02 and 0.98 for the PS/$S_{0.49}$-*r*-MMA blend gives $\chi_{hc} = 0.0035$ instead of $\chi_{hc} = 0.0076$ when the phase compositions approach 0 and 1. To truly obtain an accurate measure of the PS/$S_{0.49}$-*r*-MMA interaction parameter, it would be desirable to repeat the experiments with polymers of lower molecular weights. Results are less ambiguous with this technique if there is an observable degree of miscibility.

For system II, the $\chi_{PS/PEMA}$ values of 0.013 and 0.012, from the PS/$S_{0.47}$-*r*-EMA and PEMA/$S_{0.47}$-*r*-EMA blends, respectively, are slightly less than the $\chi_{PS/PEMA} = 0.016$ reported in the literature based on DSC measurements.[19] For PS/PBMA, we measured $\chi_{PS/PBMA} = 0.0076$. This value is lower than the $\chi_{PS/PBMA}(156\ °C) = 0.0055$ reported from neutron reflectivity measurements on dPS/PBMA bilayers.[20] However, the reflectivity-derived $\chi_{PS/PBMA}$ is based on interfacial width measurements and assumptions which are expected to underestimate $\chi_{PS/PBMA}$.[21] For system IV, we determined $\chi_{PS/P4VP} = 0.088$ and 0.092 from the PS/$S_{0.50}$-*r*-4VP and P4VP/$S_{0.50}$-*r*-4VP blends, respectively. PS/P4VP miscibility has not been as thoroughly studied as has the closely related PS/poly(2-vinylpyridine) system, for which $\chi_{AB}(150\ °C) \sim 0.15$.[22] The difference in these values could be due to the slight structural variance between P4VP and P2VP, as well as the difficulty in precisely determining χ's from extremely immiscible systems such as PS/4VP/$S_{0.5}$-*r*-4VP. Overall, the χ values determined for all systems are reasonable and support the validity of our cross-sectional microscopy technique.

Discussion

Evaluation of Cross-Sectional Microscopy Technique. From our results on 10 different homopolymer/copolymer blends, the error range in the determined phase compositions using the cross-sectional microscopy technique averaged ±7%. This uncertainty could readily be reduced in future miscibility studies. The error is primarily due to thickness variations in the doctor-bladed films. Finding an alternative process for preparing films of 5–30 μm thick would be ideal. Thickness fluctuations were particularly problematic for system IV due to the extremely low molecular weights of the homopolymer used and the high solution concentrations required to produce films of an appropriate thickness.

Cross-sectional optical microscopy allowed us to avoid a common difficulty encountered with thin film techniques such as FRES or neutron reflectivity, which is film dewetting. This phenomenon occurs when thermal fluctuations in the film surfaces increase in amplitude with increasing temperature, eventually reaching the substrate. This problem was one of the primary limitations encountered in our FRES experiments on dPS/$S_{0.49}$-*r*-MMA and dPMMA/$S_{0.49}$-*r*-MMA bilayers.[11] For both blends, anneal times and temperatures were limited due to dewetting of both the films from the substrate and from each other. Using high molecular weights can deter this phenomenon, but it will also slow

Table 2. Summary of Results

system		ϕ'_h	ϕ''_h	χ_{hc}	χ_{AB}	$(\lvert\Delta\chi_{AB}\rvert/(\chi_{AB})_{PS})$
Ia	PS-65/$S_{0.49}$−*r*−MMA	0 ± 0.07	1 ± 0.15	0.0076 ± 0.0003	0.028	26%
Ib	PMMA/$S_{0.49}$−*r*−MMA	0.11 ± 0.03	0.93 ± 0.06	0.0050 ± 0.001	0.021	
IIa	PS-129/$S_{0.47}$−*r*−EMA	0.12 ± 0.03	0.96 ± 0.06	0.0037 ± 0.0007	0.013	8%
IIb	PEMA/$S_{0.47}$−*r*−EMA	0.17 ± 0.07	0.77 ± 0.12	0.0026 ± 0.001	0.012	
IIIa	PS-156/$S_{0.50}$−*r*−BMA	0.03 ± 0.04	0.86 ± 0.09	0.0019 ± 0.0004	0.0076	0%
IIIb	PBMA/$S_{0.50}$−*r*−BMA	0.05 ± 0.04	0.86 ± 0.09	0.0019 ± 0.0002	0.0076	
IVa	PS-8/$S_{0.50}$−*r*−4VP	0.07 ± 0.01	1 ± 0.01	0.022 ± 0.002	0.088	5%
IVb	P4VP/$S_{0.50}$−*r*−4VP	0.09 ± 0.07	1 ± 0.13	0.023 ± 0.002	0.092	

Table 3. Comparison of Experimental Methods: dPS/$S_{0.49}$-*r*-MMA and dPMMA/$S_{0.49}$-*r*-MMA Miscibility

system	technique	ϕ'_h	ϕ''_h
dPS/$S_{0.49}$−*r*−MMA	cross-sectional microscopy	0.0 ± 0.06	1.0 ± 0.10
	FRES	0.01 ± 0.003	0.97 ± 0.05
dPMMA/$S_{0.49}$−*r*−MMA	cross-sectional microscopy	0.0 ± 0.09	0.97 ± 0.15
	FRES	0.07 ± 0.02	0.96 ± 0.05

the time to reach equilibrium for a blend. Film thicknesses employed for the cross-sectional microscopy experiments were 10−50 times larger than those commonly used for neutron reflectivity and FRES experiments. Films thicker than a micron are generally stable with respect to thermal fluctuations due to gravity.[23] Only one blend in our study, PBMA/$S_{0.50}$-*r*-MMA, dewet during annealing. By reversal of the bilayer geometry and placement of the PBMA at the air/polymer interface, the bilayer became stable.

Eliminating the need to deuterate one of the components in the blend to achieve phase contrast is another benefit of the cross-sectional microscopy technique. The extent to which deuteration affects miscibility in the PS/PMMA/$S_{0.49}$-*r*-MMA system is evident in both our FRES and cross-sectional microscopy experiments, as shown in Table 3. Besides their potential effects on miscibility, deuterated materials are considerably more expensive than their hydrogenated counterparts, and fewer chemical species are available. On the basis of our results, cross-sectional microscopy appears to be a viable and widely applicable technique for quantitative investigation of blend miscibility in polymer systems.

Observed Asymmetric and Symmetric Miscibility. The difference between $\chi_{AB}(A/AB)$ and $\chi_{AB}(B/AB)$ for systems I−IV, $|\Delta\chi_{AB}|/(\chi_{AB})_{PS}$, is included in Table 2 as a criteria for determining the extent of asymmetric miscibility. As observed previously,[2] the $S_{0.49}$-*r*-MMA copolymer is preferentially miscible with PMMA as compared to PS, as demonstrated by the $\chi_{PS/PMMA}$ interaction parameters differing by 26%. The data from system II suggest that the $S_{0.47}$-*r*-EMA copolymer also exhibits some degree of asymmetric miscibility in that the copolymer is more miscible with PEMA than PS. The difference in the $\chi_{PS/PEMA}$ values determined from the PS/$S_{0.47}$-*r*-EMA and PEMA/$S_{0.47}$-*r*-EMA blends is 8%. In contrast, the S-*r*-BMA and S-*r*-4VP random copolymers, systems III and IV, exhibit symmetric miscibility with their related homopolymers as the χ_{AB}'s determined from both the A/A_fB and B/A_fB blends agree within experimental error.

Table 4. Characteristics of Monomeric Units

monomer	δ (cal cm^{-3})$^{0.5}$	l (Å)[a]	v (Å^3)[b]
styrene	9.03	6.7	165
methyl methacrylate	9.23	6.4	140
ethyl methacrylate	9.03	5.65	168
butyl methacrylate	8.75	5.1	220
4-vinylpyridine	11.6	7.1	136

[a] *Polymer Handbook*, 3rd ed.; Brandrup, J., Immergut, E. H., Eds.; Interscience: New York, 1989. [b] Monomer volume calculated as v (Å^3) = 1.66[monomeric unit molar mass (g/mol)]/polymer density (g/cm^3).

Polarity and Size Effects on Miscibility. Two of our polymer blend systems (I, II) exhibit asymmetric miscibility and two (III, IV) behave as predicted by CE theory. We now compare these four systems based on monomer size and polarity differences. Table 4 lists the segment length, volume, and solubility parameters for the monomers in systems I−IV. The group contribution method for calculating solubility parameters is employed, because precise measurement of solubility parameters is difficult and literature values can vary significantly depending on experimental technique. Small's values for molar attraction constants, F_j, were used in the expression

$$\delta_i = (\rho_i \sum_j F_j)/M_i \tag{12}$$

where ρ_i is the polymer density and M_i is the monomeric unit molecular weight.[24] We now compare the asymmetric miscibility as given by $|\Delta\chi_{AB}|/(\chi_{AB})_{PS}$ to the difference between the A and B monomeric units in terms of their size and solubility

$$\frac{\Delta lv}{(lv)_{PS}} = \frac{(l_A v_A - l_B v_B)}{l_{PS} v_{PS}} \tag{13}$$

$$\frac{\Delta\delta}{\delta_{PS}} = \frac{(\delta_A - \delta_B)}{\delta_{PS}} \tag{14}$$

In parts a and b of Figure 3, $|\Delta\chi_{AB}|/(\chi_{AB})_{PS}$ for systems I−IV is plotted as a function of $\Delta(lv)/(lv)_s$ and $\Delta\delta/\delta_s$, respectively. The product lv is used as a measure of combined segment length and monomeric volume. The two systems which show asymmetric miscibility behavior are also found to have the largest difference in combined monomer volume and segment length: 20% for styrene and methyl methacrylate (I) and 14% for styrene and ethyl methacrylate (II). These findings imply that monomer size mismatch could be a contributing factor in causing asymmetric miscibility. One way to test this observation would be to perform further miscibility studies on homopolymer/random copolymer systems with larger volume and segment length differences than that found for styrene and methyl methacrylate. For instance, styrene and *tert*-butyl methacrylate differ in combined lv by 79% and should be an interesting system to investigate and compare with styrene/*n*-butyl methacrylate.

An expansion of FH theory known as the Lattice Cluster (LC) theory may also prove useful in verifying this potential link between monomer structure and miscibility.[25−30] FH theory is limited in its ability to model complex polymer interactions as it is insensitive to monomer sequence and structure, as well as chain architecture. Monomers in the standard FH lattice model are represented as structureless entities, and short-range correlations responsible for nonrandom mixing effects are not included. Developed by Freed and co-workers, the LC theory allows monomers to occupy different numbers of lattice sites, connected in a manner to mimic the related shapes and sizes of the monomers. Corrections are appended to the FH free energy equation to describe the effects of monomer packing constraints and monomer−monomer interactions. LC theory has been successful in modeling asymmetric miscibility between A/$A_{0.5}$B and B/$A_{0.5}$B homopolymer/random copolymer blends in which the monomers contain side groups and have vinyl structures with no tetrafunctional backbone units.[30] Currently, the LC theory cannot precisely model the PS/S-*r*-MMA and PMMA/S-*r*-MMA blends because of the size of the styrene and methyl methacrylate side groups. Perhaps future developments of the LC theory will provide theoretical evidence of a correlation between monomer size mismatch and miscibility in these blend systems.

We next explore the possibility that monomer polarity could be linked to asymmetric miscibility behavior. As shown in Figure 3b, the $\Delta\delta/\delta_s$ for systems I and II which do exhibit asymmetric miscibility are between the $\Delta\delta/\delta_s$ values for systems that do not exhibit asymmetric behavior. These results indicate that there is not a clear connection between asymmetric miscibility and polarity, as described by solubility parameters. However, IR spectroscopy results suggest otherwise. The $-C-O_2-R$ side group of PMMA, PEMA, PBMA, and their copolymers with styrene are expected to impart some polarity onto the polymer chains, whereas PS is nonpolar. A shift or broadening of the carbonyl peak in polymers provides evidence of molecular interactions driven by such polarity effects.[31] Figure 4 shows the IR spectra for PMMA, $S_{0.49}$-*r*-MMA, $S_{0.47}$-*r*-EMA, and $S_{0.50}$-*r*-BMA in the wavenumber region 1650−1800 cm^{-1}. The carbonyl stretching frequency, in the absence of hydrogen bonding, is found at 1730−1750 cm^{-1}.[31] Hydrogen bonding makes stretching of the C=O bond easier, and is evidenced in the IR spectra by a shift in the carbonyl peak to lower wavenumbers. The carbonyl peaks for PMMA and $S_{0.49}$-*r*-MMA are broad and show an overlap of two peaks, at 1743 and 1714 cm^{-1} for PMMA and at 1740 and 1715 cm^{-1} for $S_{0.49}$-*r*-MMA. These double peaks suggest that both free and associated carbonyl groups are present in the polymer samples. The carbonyl region for $S_{0.47}$-*r*-EMA shows a primary peak at 1734 cm^{-1}, close to the value expected for a free carbonyl group, but there is still a shoulder to the peak at ~1710 cm^{-1} that suggests some association between the carbonyl groups of the copolymer is occurring. In contrast, the $S_{0.50}$-*r*-BMA spectra shows only one peak, at 1735 cm^{-1}, which indicates the absence of carbonyl group associations. This result is reasonable, because the increased bulkiness of the butyl side group relative to the methyl or ethyl side groups increases the steric hindrance near the carbonyl group. The general trends observed in these results support the idea that intramolecular and intermolecular associations between polar groups could be a factor responsible for asymmetric miscibility. Copolymers such as $S_{0.49}$-*r*-MMA and $S_{0.47}$-*r*-EMA within which carbonyl groups associate would be expected to exhibit enhanced miscibility with homopolymers that contain carbonyl groups, such as PMMA and PEMA, but not PBMA. Conversely, $S_{0.49}$-*r*-MMA and $S_{0.47}$-*r*-EMA would be less likely to mix easily with PS as the number of carbonyl associations would need to be reduced, an enthalpically unfavorable condition.

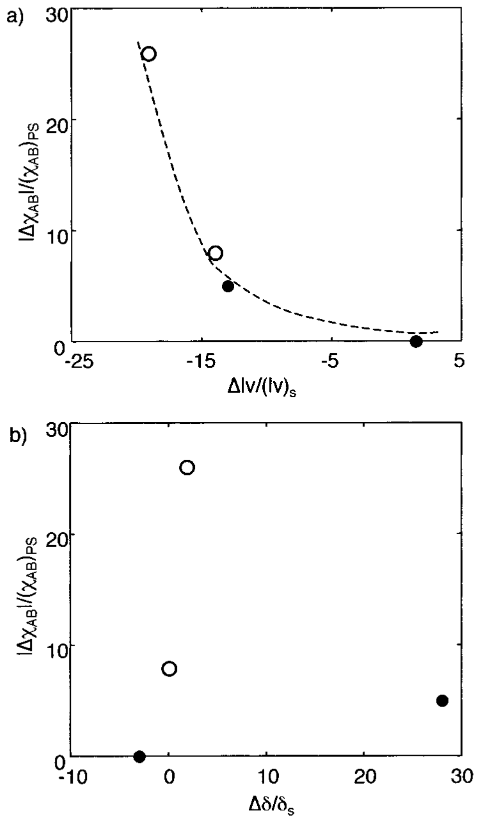

Figure 3. Relative difference in χ_{AB} determined from the A/A_fB and B/A_fB blends for systems I−IV: (a) plotted as a function of differences in monomeric size, $\Delta lv/(lv)_s$; (b) plotted as a function of differences in monomeric solubility, $\Delta\delta/\delta_s$. Open circles are for systems I and II, which show asymmetric miscibility; filled circles are for systems III and IV, which do not show asymmetric miscibility.

Conclusions

We have developed a new technique for investigating polymer miscibility, cross-sectional microscopy, based on the principle of using linearized mass balances to determine coexistence compositions. This technique was found to be a viable and widely applicable method for investigating polymer blend miscibility. There is no need to deuterate or otherwise label blend components or the interfaces in order to achieve contrast between phase-separated regions. Results obtained using cross-sectional microscopy to study the dPS/dPMMA/$S_{0.49}$-*r*-MMA system were in good agreement with results obtained from previous FRES experiments. By using films 5−30 μm thick for the microscopy study instead of 50−500 nm for neutron reflectivity or FRES, dewetting is avoided during the annealing process of sample preparation. Improvements in sample preparation techniques could increase the accuracy of cross-sectional microscopy measurements of coexistence compositions.

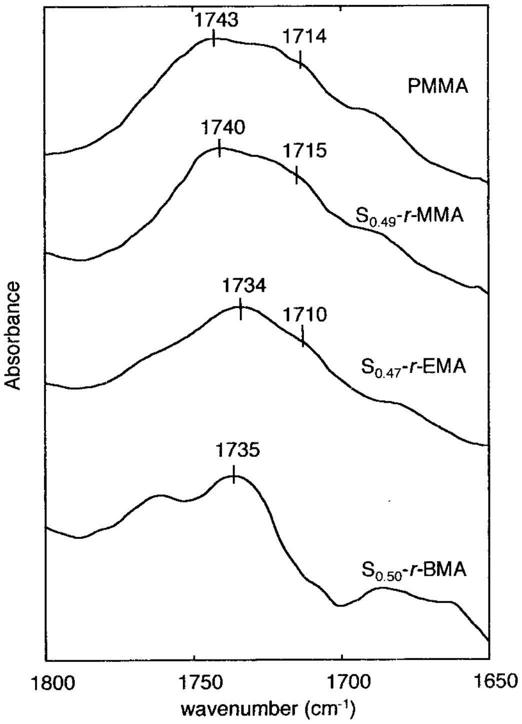

Figure 4. Infrared spectra from PMMA, $S_{0.49}$-*r*-MMA, $S_{0.47}$-*r*-EMA, and $S_{0.50}$-*r*-BMA. PMMA, $S_{0.49}$-*r*-MMA, and $S_{0.47}$-*r*-EMA show both associated and free carbonyl groups, while $S_{0.50}$-*r*-BMA shows only free carbonyl groups.

The asymmetric miscibility of the PS/PMMA/$S_{0.49}$-*r*-MMA system reported previously has been verified in this study. The symmetric $S_{0.49}$-*r*-MMA copolymer exhibited preferential miscibility with PMMA, as seen in the higher interaction parameter determined for PS/$S_{0.49}$-*r*-MMA as compared to the value determined for PMMA/$S_{0.49}$-*r*-MMA. A second polymer system, PS/PEMA/$S_{0.47}$-*r*-EMA, showed similar asymmetric miscibility, where the random copolymer was more miscible with PEMA than with PS. Two other copolymers investigated in this study, $S_{0.50}$-*r*-BMA and $S_{0.50}$-*r*-4VP, were equally miscible with both of their related homopolymers and behaved as predicted by the Copolymer Effect theory. A possible connection between monomer size and asymmetric miscibility was observed, as the styrene/methyl methacrylate and styrene/ethyl methacrylate pairs have the largest combined size and segment length mismatch ($\Delta l v/l v_S$) of the four hydrogenated systems studied. Further studies of homopolymer/copolymer systems with size differences greater than that of styrene and methyl methacrylate is recommended in order to verify this observed trend.

A potential link between polymer polarity and asymmetric miscibility was revealed through infrared spectroscopy experiments. The $S_{0.49}$-*r*-MMA and $S_{0.47}$-*r*-EMA spectra revealed a broadening of the carbonyl stretching peak indicative of polar group association. This peak broadening was not observed for the $S_{0.50}$-*r*-BMA copolymer, suggesting that the butyl side group is too bulky to allow for carbonyl association. More thorough IR experiments, including studies of blends of these copolymers with their related homopolymers, could provide further information to confirm these trends.

References and Notes

(1) Galvin, M. E. *Macromolecules* **1991**, *24*, 6354.
(2) Winey, K. I.; Berba, M. L.; Galvin, M. E. *Macromolecules* **1996**, *29*, 2868.
(3) Kulasekere, R.; Kaiser, H.; Ankner, J. F.; Russel, T. P.; Brown, H. R.; Hawker, C. J.; Mayers, A. M. *Macromolecules* **1996**, *29*, 5493.
(4) Kambour, R. P.; Bendler, J. T.; Bopp, R. C. *Macromolecules* **1983 16**, 753.
(5) Brinke, G. ten; Karasz, F. E.; MacKnight, W. J. *Macromolecules* **1983**, *16*, 1827.
(6) Paul, D. W.; Barlow, J. W. *Polymer* **1984**, *25*, 487.
(7) Flory, P. J. *Principles of Polymer Chemistry*; Cornell University Press: Ithaca, NY, 1953.
(8) Bates, F. S.; Schultz, M. F.; Rosedale, J. H.; Almdal, K. *Macromolecules* **1992**, *25*, 5547.
(9) Coleman, M. M.; Serman, C. J. Bhegwagar, D. E.; Painter, P. C. *Polymer* **1990**, *31*, 1187.
(10) Graessley, W. W.; Krishnamoorti, R.; Reichart, G. C.; Balsara, N. P.; Fetters, L. G.; Lohse, D. J. *Macromolecules* **1995**, *26*, 1260.
(11) Pellegrini, N. N.; Composto, R. J.; Winey, K. I., submitted to *J. Polym. Sci.: Polym. Phys.*
(12) Galvin, M. E.; Heffner, S.; Winey, K. I. *Macromolecules* **1994**, *27*, 3520.
(13) Balazs, A. C.; Sanchez, I. C.; Epstein, I. R.; Karasz, F. E.; MacKnight, W. *Macromolecules* **1985**, *18*, 2188.
(14) Balazs, A. C.; DeMeuse, M. T. *Macromolecules* **1989**, *22*, 4260.
(15) *Copolymerization*; Hamm, G. E., Ed.; Interscience: New York, 1964.
(16) Bovey, F. A. *J. Polym. Sci.* **1962**, *62*, 197.
(17) Pellegrini, N. N. Ph.D. Thesis, University of Pennsylvania, 1999.
(18) Callaghan, T. A.; Paul, D. K. *Macromolecules* **1993**, *26*, 2439.
(19) Chen, J.; Goh, S. H.; Lee, S. Y.; Slow, K. S. *Polymer* **1994**, *35*, 1477.
(20) Siqueira, D. F.; Schubert, D. W.; Erb, V.; Stamm, M.; Amato, J. P. *Colloid Polym. Sci.* **1995**, *273*, 1041.
(21) Schubert, D. W.; Abeta, V.; Hack, T.; Stamm, M.; Soil, W. *Macromolecules* **1995**, *28*, 2519.
(22) Dai, K. H.; Kramer, E. J. *Polymer* **1994**, *35*, 157.
(23) Reiter, G. *Langmuir* **1993**, *9*, 1344.
(24) *Polymer Handbook*, 3rd ed.; Brandrup, J., Immergut, E. H., Eds.; Wiley (Interscience): New York, 1989.
(25) Dudowicz, J.; Freed, K. F. *Macromolecules* **1991**, *24*, 5076.
(26) Dudowicz, J.; Freed, M. S.; Freed, K. F. *Macromolecules* **1991**, *24*, 5096.
(27) Dudowicz, J.; Freed, K. F. *Macromolecules* **1996**, *29*, 7826.
(28) Dudowicz, J.; Freed, K. F. *Macromolecules* **1996**, *29*, 8960.
(29) Dudowicz, J.; Freed, K. F. *Macromolecules* **1997**, *30*, 5506.
(30) Dudowicz, J.; Freed, K. F. *Macromolecules* **1998**, *31*, 5094.
(31) Pearce, E. M.; Kwei, T. K. *Polymer Solutions, Blends and Interfaces* Elsevier Science Publishers: Amsterdam, 1992.

MA991151T